



Covestro Coatings for Optical Fibers

Digitalization needs are evolving rapidly, and fiber performance is key to the reliability and durability of current and next generation mobile networks moving toward 5G.

Market leader Covestro uses unique technical capabilities to identify solutions and deliver high performance fiber coatings for the world's telecommunications market.

Our innovative solutions are built on 40 years of technical experience, research and development and close partnerships that enable the sustainable success of fiber makers, cable producers and telecom partners.

UV-curable High Temperature Resistant Dual Layer Coating System for Specialty Optical Fiber Applications

Huimin Cao, Keegan Orendorff, Todd Anderson, Eric Urruti

Covestro LLC, Elgin, IL, 60120, USA

+1-224-4020950 · huimin.cao@covestro.com

Abstract

Fiber optics technology has been applied into more and more varieties of specialty applications, where the optical fibers/cables are routinely used under harsh environments of high temperatures. The development of a reliable high temperature resistant coating system that can also meet the requirement of fast draw speed of fiber drawing process is highly desirable. In this work, a UV-curable dual layer acrylate coating system has been developed closely matching high temperature thermal stability of a commonly used UV-curable high temperature resistant single coat demonstrated with excellent field performance in the past 10 years. The high temperature thermal stability of the dual layer coating system was evaluated using weight loss by Thermogravimetric Analysis (TGA), as well as mechanical property characterization by Dynamic Mechanical Analysis (DMA) of film samples, in comparison with a standard telecom grade dual layer coating system and the high temperature resistant single coat. The film study from the newly developed dual layer coating system has shown optimized balance between high temperature thermal stability similar to the single coat and improved mechanical properties over single coat as a soft/hard dual layer coating system.

Keywords: optical fiber coating; high temperature resistance; Arrhenius study; lifetime prediction; specialty fiber applications.

1. Introduction

The demand of optical fibers in specialty applications such as automotive, aerospace, optical power composite cable, sensors, oil & gas rigs, high power lasers...has been growing in recent years. These applications require long term durability at mid-high temperature range, or mid-term durability at high temperature range. Conventional high temperature resistant polymers such as silicones or polyimides as thermal curable materials involve complex processing such as solvent removal requiring slow draw speed of optical fiber, which becomes a limiting factor for actual application. Extensive efforts have been reported developing acrylate-based UV-curable high temperature resistant coatings supporting the high drawing speed of optical fiber manufacturing process [1-5].

A high temperature resistant single coat product DF-0009 was introduced to the industry in 2009, based on the work reported by Murphy *et al* [1,2]. From the mechanism of polymer degradation, the weakest link to thermal oxidation and thermal pyrolysis in the commonly used UV curable urethane acrylate compositions for optical fiber coating was identified to be urethane linkage of carbamate moiety, as well as the poly(propylene glycol) moiety in the typical urethane acrylate structure [1]. DF-0009 successfully adopted a non-urethane acrylate composition with significantly improved high temperature resistance. This coating with modulus designed in the medium level ~700MPa as a single coat material has been proven supporting optical fiber applications in long term use at high temperature range 100-150°C, or short term use at extreme temperature range 150-200°C. Compared with overall optical and mechanical performance of a standard optical fiber dual

layer coating system, intrinsic gap remains with DF-0009 as a single coat system. Single coat is much more difficult to strip, due to the critical bucking force of a 60µm thick single coat is much higher than a 30µm secondary coating in a dual layer coated fiber (soft primary coating modulus contribution negligible, only adhesion to glass having influence to strip force). Another important property is microbending performance: single coat is much worse microbending protection than standard dual layer coating system which provides the combined cushioning and shielding effects against external stress perturbation from the soft inner primary coating + hard outer secondary coating design.

High temperature resistant dual layer UV-curable acrylate coatings have been reported in the past [3-5]. While the high temperature thermal stability has shown greatly improved over conventional coatings with continuous use temperature predicted for 20yrs lifetime improved from ~80°C to ~110°C [4], the gap to DF-0009 single coat reported at 130°C [5] is still significant.

In this paper, a newly developed high temperature resistant dual layer UV-curable coating system is introduced, consisting of primary coating HT-P and secondary coating HT-S. The film study showed close match of high temperature thermal stability of HT-P/HT-S dual layer coating system to DF-0009 single coat, while providing improved mechanical properties as soft/hard dual layer coating system.

2. Experiments

2.1 Coating Film Sample Preparation

Each coating sample was drawn down by Bird bar applicator at a nominal 25µm (1mil) film thickness on glass plate for TGA tests, or 75µm (3mil) film thickness for DMA or tensile tests. Dual layer coating samples for TGA were prepared by first draw down and cure a 1mil layer of primary coating and then use 2mil drawdown bar applying 1mil thickness of secondary coating layer on top of primary coating and cure again. The TGA samples were cut into 0.5cm squares and a single piece was placed into the platinum sample pan for each TGA test.

The sample curing was conducted on Fusion Light Hammer10 conveyor system of Heraeus Noblelight with 10 inch 600 W/in D lamp, purged with 15 ft³/min N₂. The standard curing dose measured by radiometer ILT800 was 1J/cm². The film samples were then conditioned in a temperature/humidity controlled room at 23°C/50%RH.

2.2 Thermal Aging

The aging of 3mil cured coating samples was conducted in Blue M mechanical oven with horizontal air flow which assures uniform thermal condition. The samples after aging were reconditioned in the temperature/humidity controlled room at 23°C/50%RH for >16hrs before conducting weight measurements or DMA testing.

2.3 Thermogravimetric Analysis (TGA)

Thermogravimetric analysis of film samples was conducted using TA Instruments Hi-Res TGA 2950 Thermogravimetric Analyzer.

2.3.1 Dynamic TGA. Dynamic TGA of temperature sweep was set with standard condition of 10°C/min heat rate and 50L/min dry air flow, except for special conditions of different flow rates of air or in N₂ as specified.

2.3.2 Isothermal TGA. For isothermal TGA test, the program sequence was set to first equilibrium at 25°C for 1 min; then ramp up temperature with rapid heating rate of 200°C/min to the target temperature, in order to minimize the weight loss during this ramping period; finally isotherm at the target temperature for a specified time period. This entire process was under the condition of 50L/min dry air flow.

2.4 Dynamic Mechanical Analysis (DMA)

Dynamic mechanical analysis was conducted using RSA-G2 Solids Analyzer from TA Instruments.

2.4.1 DMA Temperature Sweep of Film Samples. Before conducting the temperature sweep, moisture was removed from the test sample by subjecting the test samples to a temperature of 80°C in a N₂ atmosphere for 5 minutes. The sample was then cooled under liquid N₂ condition to -60°C and the temperature sweep from -60°C to 160°C was conducted. The oscillation frequency was set at 1.0 radian/s. The results of storage modulus E', loss modulus E'' and Tanδ (=E''/ E') were plotted. The temperature of tanδ peak position was reported as Tanδ T_g, as the glass transition temperature from polymer glassy state to rubbery state. The minimum value at the rubber plateau E' was reported as equilibrium modulus E₀.

2.4.2 Primary In-Situ Modulus of Glass Fibers. A detailed description of the test method and data processing methodology for primary in-situ modulus on glass fiber was introduced in previous paper [6], using DMA machine shear sandwich mode to measure shear modulus G_p of primary coating under 1 radian/s frequency, and converting to tensile modulus E_p as the primary in-situ modulus.

2.4.3 Secondary In-Situ Modulus of Glass Fiber. The coating tube samples for secondary in-situ modulus were prepared by stripping ~2-5cm length of the dual layer coating tube out of the glass fiber when the coating became stiff after dipping in liquid N₂. DMA machine was used to measure the storage tensile modulus E' of the coating tube sample. With secondary coating >1000 times higher modulus than primary coating, the contribution from primary coating modulus in tensile mode testing of the coating tube is negligible. The measured tensile storage modulus E', with geometry entered as a rod with cross section area equivalent to the secondary coating hollow cylinder, is reported as the secondary in-situ modulus.

3. Results and Discussion

3.1 Thermal Degradation of Polymers

Harsh environmental factors such as solar radiation, temperature, and humidity could act interactively in the polymer degradation process. In the high temperature specialty fiber applications, thermal degradation of polymer coatings at high temperature in air environment is the main culprit. Direct thermal decomposition (or thermolysis) of breaking chemical bonds by heat only occurs at the decomposition temperatures, which are typically very high (>300°C), when the thermal energy exceeds the bond association energy of various chemical bonds of the substance. The dominant degradation mechanism for polymers in air environment at a temperature lower than decomposition temperature is thermal oxidation.

Figure 1 illustrates a general free radical thermo-oxidative degradation mechanism for polymers [7]. The role of O₂ in this

degradation process is critical: 1) free radical propagation through forming peroxide radical RO₂• 2) auto-acceleration by chain-branching through hydroperoxide decomposes to form more radicals, leading to an increase in the oxidation rate. As the end results of these free radical chain reactions, two major effects are directly responsible for the polymer chemical structure breakdown resulting in physical property degradation such as material weakening and material embrittlement (the loss of tensile strength, elongation, toughness), cracking, chalking, color changing, etc. The two major effects are 1) chain scission: breaking long polymer chains into short chain fragments causing weakening of the material. The polymeric oxy radical RO• is very reactive and readily lead to β-chain scission reaction. 2) crosslinking: the termination by recombination of two radicals results in an increase of crosslinking density. Because the polymer structure already broke down into short chain fragments, the crosslinking of these short chain fragments leads to brittle structure, prone to fracture failure such as cracking and chalking.

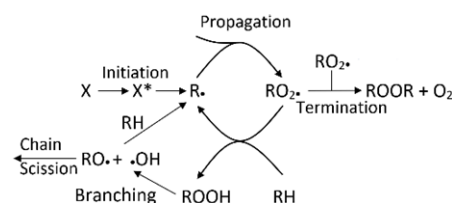


Figure 1. General thermo-oxidative degradation mechanism for polymers

3.2 Failure Mode Analysis on a Standard Coating Coated Fiber after High Temperature Aging

In order to demonstrate different failure modes of conventional telecom grade optical fiber after high temperature degradation, a fiber with a commonly used standard dual layer coating system Std-P/Std-S was placed in 180°C or 200°C oven and the property changes being monitored for 5 days.

The first change observed was the primary coating turned much softer into a gel-like material after just 1 day of 180°C aging. Figure 2a is the fiber after 1 day 180°C aging, with light pressure manually pressing on the fiber, already created many big cavity/delamination sites in the primary coating. The fiber can also easily tube off by hands, leaving sticky gel-like coating residue on glass. This failure mode represents a chain scission dominated stage in soft primary coating, breaking down crosslinking structure depolymerizing into a gel-like material. Figure 2b is the fiber sample winded in small coil of ~8cm diameter during aging. When sample taken out after 5 days of 180°C, the glass was seen shifted position significantly inside of the primary coating that all primary coatings flowed to inner side of the fiber coil. This again is an indication that primary coating lost elasticity due to chain scission and the glass easily crept inside of the disintegrated primary coating under the low level winding stress.

Interestingly, this fiber after 5 days of 180°C aging, despite the color turning much darker than earlier days, the coating was no longer easily tubing off, but became very difficult to strip off the glass, indicating at this point the primary coating is no longer a gel-like material. This as explained in the last section, is when the degradation process progressed from early chain scission dominated stage to finally crosslinking dominated termination stage. The direct proof can be found in Figure 3. In-situ modulus of the primary coating (measured at room temperature) with 180°C aging quickly decreased from the initial value of 0.5MPa to 0.3MPa after just 3hrs, then dropped to 0.01MPa after 1 day, consistent with modulus level from

a very weakly crosslinked gel, then slightly increased to 0.02MPa after 2 days, followed by significant increase to 0.3MPa after 3 days and 3.4 after 5 days. This trend of primary coating first softened and disintegrated into a gel then hardened to a much higher modulus brittle material is expected to also apply to lower temperature aging conditions, just taking longer time to go through these different stages. The first stage of chain scission is most risky with regard to fiber performance issues, due to easy formation of delamination and cavitation in primary coating after losing integrity, plus more severe weight loss of primary coating than secondary coating creating high tri-axial tensile stress in primary coating adding more risk for defect formation.

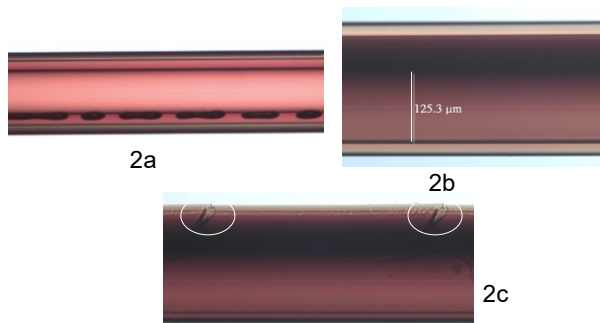


Figure 2. Failure modes of a standard dual layer coating coated fiber after high temperature aging: (2a) 1 day 180°C aged fiber after manual handling. (2b) fiber sample in ~8cm diameter coil after 5 days 180°C. (2c) 5 days 200°C aged fiber after manual handling

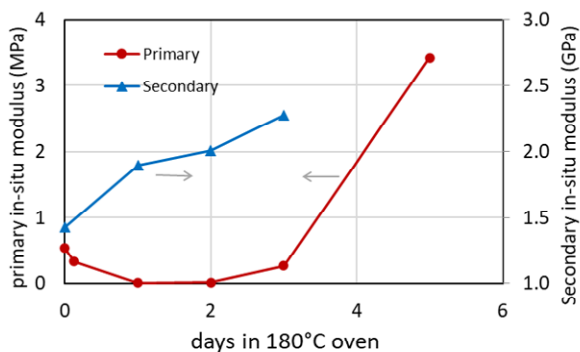


Figure 3. Change of primary and secondary in-situ modulus vs. time of 180°C oven aging for a standard dual layer coating coated fiber

Secondary coating as a harder material with much higher crosslink density than primary coating, although undergoes the same failure mechanism including both chain scission and crosslinking, no clear softening stage was observed as in primary coating, crosslinking dominated and caused embrittlement of the secondary coating. Figure 2c shows cracking started from the secondary layer with 5 days of 200°C aged fiber after manual bending. From Figure 3, the measured secondary in-situ modulus was confirmed to continuously increase with aging time. Modulus increase from initial 1.3GPa to 2.3GPa after 3 days 180°C is still within acceptable range, however, the elongation at break is expected significantly reduced after high temperature aging, causing severe brittleness easy to crack. No secondary in-situ data for the 5 days 180°C fiber was obtained, because the coating was so brittle that it could not hold integrity when being stripped under liquid N₂.

3.3 Design of UV-Curable High Temperature Resistant Dual Layer Coating System

Based on the failure mode analysis of the standard coating coated fiber which is representative of general failure modes in all conventional urethane acrylate coating coated fibers, the design target of the new dual layer high temperature resistant UV-curable coating system was set to be 1) primary coating: prevent severe chain scission to avoid disintegration into a gel-like material under high temperature applications. 2) secondary coating: prevent severe crosslinking to avoid detrimental embrittlement under high temperature applications. Among these two objectives, primary coating is much more challenging due to low crosslink soft coating intrinsically much more vulnerable to lose network integrity than high crosslink coating after thermal degradation.

The chemistry of both coatings is designed to be non-urethane acrylate based UV-curable material, as proven by the superior thermal stability of DF-0009, successfully used as a high temperature single coat product for specialty applications at 100-200°C mid to high temperature ranges with different durations.

As a dual layer soft/hard coating system design, as shown in Table 1 (tensile modulus from tensile tester, Tanδ T_g from DMA), the primary coating HT-P is designed at medium low modulus level of 5MPa for optimizing both thermal stability at high temperature and mechanical properties. Even though the modulus level is above the standard telecom grade primary coating such as Std-P at 1.2MPa, the improvement on microbending performance over single coat DF-0009 should still be significant; furthermore, the strip force of this dual layer coating is expected to be much lower than single coat due to secondary coating layer thickness as a controlling factor for strip force is only half of single coat coated fiber. The secondary coating HT-S is designed with a high modulus matching standard coating Std-S, for achieving much improved microbending performance than single coat, while T_g is designed to be much lower than Std-S, similar to DF-0009 level in order to reduce brittleness after high temperature aging.

Table 1. Main mechanical property comparison of the newly developed coatings vs. controls

	Tensile Modulus (MPa)	Tanδ T _g (°C)
DF-0009	700	48
HT-P	5	6
HT-S	1200	54
Std-P	1.2	-26
Std-S	1200	90

3.4 Dynamic TGA Results

TGA weight loss is a common characterization method for monitoring the progression of polymer degradation under high temperature conditions. The degree of polymer degradation directly associates with the formation and release of small molecule volatile gases as the depolymerization products from the degradation process. TGA is an accelerated method to monitor this process through precisely measuring weight loss under precisely controlled preset conditions. For Dynamic TGA temperature sweep test, the conditions of heat rate and air flow rate were set arbitrarily, which is for the purpose of relative comparison of different materials under the same condition. Dynamic TGA conducted at different heat rates through Arrhenius equation with failure criteria set, such as 25% weight loss, was commonly applied as a methodology for lifetime prediction [3-5]. Another variable that can influence the TGA weight loss rate is the gas flow rate. Figure 4 shows an example from DF-0009. While it is easily understandable the onset temperature under 50L/min of air is much lower than under 50L/min of N₂, another proof thermal

oxidation dominates the degradation when O₂ is present, it is also clear that the flow rate of air strongly influences the onset temperature. Slower the air flow rate, more closer the curve shifted to the curve in N₂. The likely cause is high-temperature oxidation of these thin small specimens is so rapid, i.e. the O₂ consumption is so rapid, that the local O₂ surrounding the sample could be depleted if the air flow rate is too slow, not able to maintain equilibrium concentration in the coating during the reaction. It is unclear what level of air flow rate setting can better represent the field environment of optical fiber cable in the specialty applications.

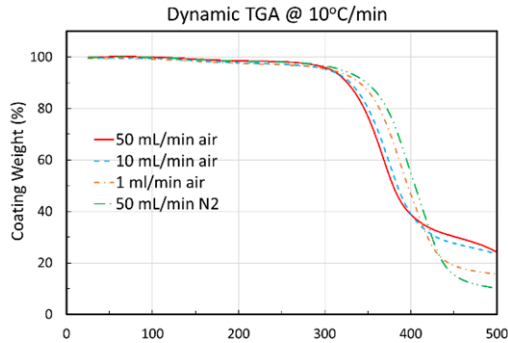


Figure 4. Dynamic TGA of DF-0009 in N₂ or air with different flow rates

Regardless of the uncertainty related to predicting absolute lifetime based on TGA results influenced by the condition setting, the relative trend between different materials in terms of thermal stability and long term durability using TGA comparison is expected to be valid. Figure 5 compares the temperature ramp TGA curves of the 5 coatings, with onset temperature listed in Table 2. It is clear that HT-S matches the thermal stability of DF-0009 with slight increase on onset temperature, or known as oxidation induction temperature (OIT). Primary coating HT-P showed the %weight loss occurred at lower temperature range more than Std-S, but only for the initial 10% weight loss. The onset temperature to sharp drop region is much higher than Std-S and actually similar to DF-0009. This is not trivial considering HT-P is designed with modulus 240 times lower than a regular secondary coating such as Std-S as well as having a much lower T_g.

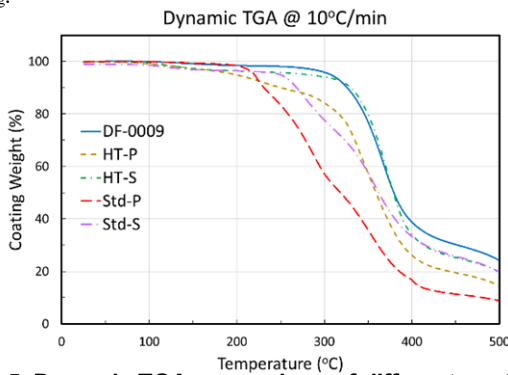


Figure 5. Dynamic TGA comparison of different coatings

3.5 Isothermal TGA Results and Lifetime Prediction

Both dynamic TGA at different heat rates and isothermal TGA at different temperatures can be used for Arrhenius lifetime prediction. In this work, isothermal TGA was used at high temperature range up to 300°C for prediction of coating lifetime into lower temperature range ≤200°C.

As an example, Figure 6 compares the residual coating %weight vs. time for the 5 coatings at 260°C. The trend of thermal stability from isothermal TGA is in good agreement with dynamic TGA, HT-S slightly better stability than DF-0009; HT-P confirmed to be longer lasting than Std-S due to the much slower rate of weight loss despite the initial lower weight possibly from fast losing of some volatile components in HT-P. The long term thermal stability of HT-P at application temperature is expected to be better than Std-S, and of course significantly better than Std-P.

Isothermal TGA curves at a set temperature can also provide some information on the complex material thermal degradation reaction kinetics. A general mathematical expression of the rate equation is often described as in Equation 1,

$$\frac{dc}{dt} = k \prod_i c_i^{m_i} \quad (1)$$

where k is the reaction rate constant, c_i is the molar concentration of reactant i and m_i is the partial order of reaction for this reactant. The exact reaction kinetics can be very complex and understandably very different for coatings designed with different chemistries and different network structures. From Figure 6, DF-0009 and HT-S both are close to a linear decreasing function with time, which indicates a pseudo zero order kinetics. This linear weight drop was tested valid till ~60% residue weight then curved to a much slower rate. This pseudo zero order kinetics of DF-0009 and HT-S indicates the oxidation reaction in these coatings are sufficiently slow that the molar concentrations of the reactive groups are not significantly changing with time until later stage. In contrast, the other three coatings showed faster non-linear weight loss, especially Std-P dramatically faster due to the severe chain scission dominated reactions. These curves, although do not fit perfectly into 1st order kinetics of exponential decay or 2nd order kinetics of reciprocal decay curves, it is for certain strongly dependent on the fast depletion of the reactive moieties.

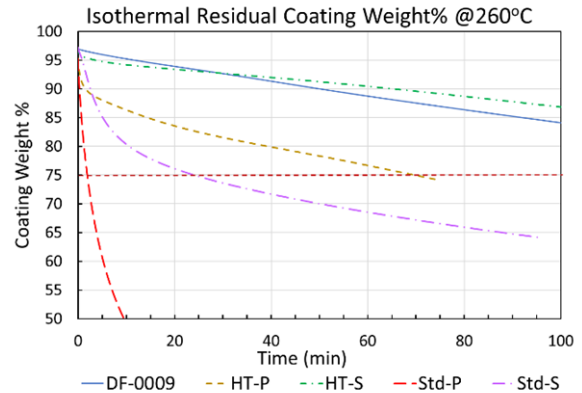


Figure 6. Isothermal TGA comparison of high T and standard coatings at 260°C

Arrhenius equation as in Equation 2 is the commonly used methodology for lifetime prediction of a material at a specified application temperature, or the upper use temperature for a specified lifetime, through conducting accelerated experiments at higher temperature range. Any method using a short term test plotting a property change vs. time under certain accelerated aging condition in attempt to fit degradation reaction constant k , and use the calculated k for the Arrhenius prediction is risky, due to the complex kinetics of different materials not possible to reliably capture k in a short term test. The proper approach as demonstrated in the previous work [1-5] is through measuring time duration reaching a set failure criteria,

lifetime τ . The failure criteria as arbitrarily set [3-5] for TGA weight loss is 25%, where the volume shrinkage and material property change at this level of weight loss are considered significant enough to cause performance failure. Since τ is directly proportional to $1/k$, the Arrhenius equation can be rewritten to Equation 3, where the activation energy E_a can be derived from multiplying the slope of the $\ln\tau$ vs $1/T$ Arrhenius linear plot with gas constant R . The intercept combines the $\ln(\text{frequency factor } A)$ and other kinetic parameters.

$$k = Ae^{-E_a/RT} \quad (2)$$

$$\ln\tau = \text{intercept} + E_a/RT \quad (3)$$

The Arrhenius plots at 25% weight loss of the 5 coatings as shown in Figure 7 clearly illustrates the much superior high temperature stability of HT-P and HT-S, compared to the corresponding conventional coating Std-P and Std-S, with HT-P actually reaching longer lifetime than HT-S which is very impressive as a much softer coating. HT-S is slightly more durable than DF-0009 due to the higher crosslink density design. It should be noted that for Std-P and Std-S, the Arrhenius curves were found not linear at the temperature range of 230°C to 300°C, not valid for lifetime prediction into lower temperatures. Further tests at lower temperature down to 160°C for Std-P and 180°C for Std-S were able to obtain better linear relationship and used for lifetime prediction. This is an indication for urethane acrylate based conventional chemistry, multiple reactions of different moieties such as urethane linkage, PPG linkage, acrylate linkage, likely have different rate constant k , and their contributions in the overall degradation reaction varying at different temperature ranges. Closer the testing temperature range to the application temperature range, more reliable the lifetime prediction will be.

Figure 8 is the plot of predicted lifetime comparison of the 5 coatings based on the 1mil film isothermal TGA test. The activation energy E_a , intercepts, and the predicted upper temperatures for 20yrs or for 1yr continuous use for the coatings are summarized in Table 2. It should be noted that these absolute values of the lifetime or upper temperature should not be directly taken as for coated fibers. Even based on the same TGA conditions, the film samples are known to have faster weight loss than coating layer on fiber likely because the coating on fiber only having outer surface exposed to air, while the film sample having all surfaces exposed to air (bottom surface not sealed to the pan). A reference data point is DF-0009, with single coating coated fiber TGA Arrhenius test, the upper temperature for 20yrs continuous use was reported to be 130°C [5], while the prediction based this film study is 118°C. All the lifetime or upper temperature prediction based on the film study are expected to be lower than actual coated fibers. The relevant trend from film sample study should still reliably represent the trend from coated fibers. The activation energy of conventional urethane acrylate based primary coating such as Std-P found to be significantly lower than other coatings once again demonstrates conventional primary coating is the weakest link most vulnerable to severe degradation. HT-P activation energy raised to similar level to secondary coatings or single coat is a strong evidence HT-P is a radically improved primary coating with regard to high temperature stability than Std-P, with upper temperature for 20yrs raised ~40°C higher.

In order to more closely simulate the coating behavior on fiber, dual layer coating samples of 1mil+1mil were tested in comparison with 2mil sample of DF-0009. Figure 9 gives an example of the dual layer coating weight loss behavior vs. single layer. The dual layer curve of residue weight% is higher than the average of 1mil individual layer of HT-P and HT-S. The simple reason is dual layer only having secondary top surface and primary bottom surface exposed to air,

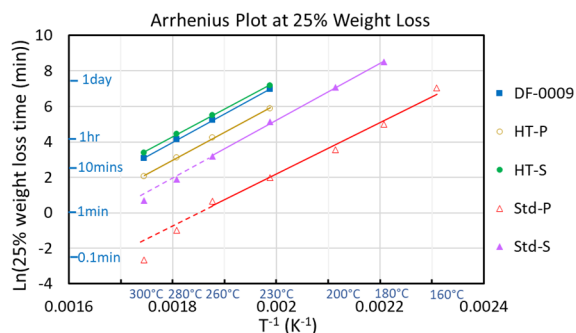


Figure 7. Arrhenius plots of high T and standard coatings from 1mil film samples

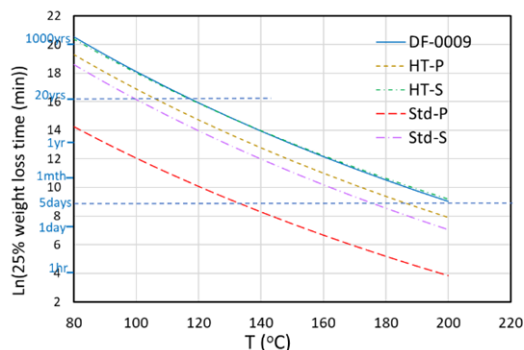


Figure 8. Predicted lifetime (based on 25% weight loss) of high T and standard coatings from 1mil film samples

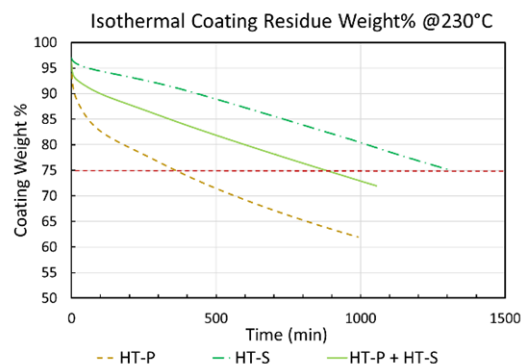


Figure 9. Isothermal TGA comparison of 1mil single layer vs. 1mil+1mil dual layer coatings at 230°C

while single layer film sample having all surfaces exposed to air. This causes the dual layer results to align more with the secondary coating.

Figure 10 and 11 are the Arrhenius plot and the predicted lifetime from the dual layer system in comparison with 2mil DF-0009. Attributed from the slightly longer durability of HT-S than DF-0009 and strong thermal performance of HT-P, the HT-P/HT-S dual layer coating system was tested to match DF-0009 single coat high temperature durability very closely, with lifetime and upper temperature prediction virtually the same level. In contrast, the dual layer conventional urethane acrylate coating system Std-P/Std-S despite the durability being much longer than Std-P alone, the fitted E_a somehow is even lower than primary coating alone, causing the dual layer prediction similar to the primary Std-P. This is not expected to be real as dual layer is supposed to be slower weight loss than single primary layer alone as the total weight loss% is based on the combined two layers. Much longer test run into lower temperature

region is needed to get a more realistic E_a for the Std-P/Std-S dual layer system for predicting into the application temperatures. There is indication the curve might be getting into a higher slope from 160°C and below. Regardless the uncertainty of the lifetime prediction of the standard coating system, primary coating being the weakest link in the conventional dual layer coating system, as the key factor responsible for the poor thermal stability of the coated fiber at high temperatures is generally true, as demonstrated in section 3.2.

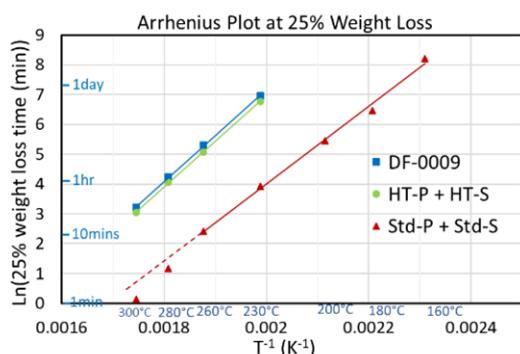


Figure 10. Arrhenius plots of high T and standard coatings from dual layer or DF-0009 2mil film samples

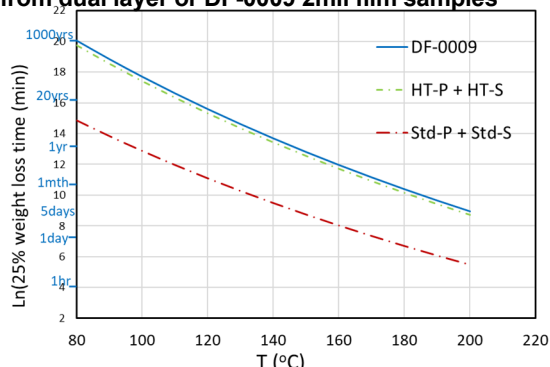


Figure 11. Predicted lifetime (based on 25% weight loss) from dual layer or DF-0009 2mil film samples

Table 2. Dynamic TGA onset temperature and Isothermal TGA Arrhenius fit and prediction

Coatings (1mil sample)	Dynamic TGA	Isothermal TGA Arrhenius Prediction			
	Onset T (°C)	E_a (kJ/mol)	Intercept	Upper T for 20yrs (°C)	Upper T for 1yr (°C)
DF-0009	328	133	-24.9	118	148
HT-P	320	132	-25.5	107	136
HT-S	334	130	-23.8	117	149
Std-P	214	120	-26.8	64	90
Std-S	255	134	-26.9	100	128

Coatings (2mil single or 1mil+1mil dual layer)	Isothermal TGA Arrhenius Prediction			
	E_a (kJ/mol)	Intercept	Upper T for 20yrs (°C)	Upper T for 1yr (°C)
DF-0009	128	-23.7	114	146
HT-P+HT-S	127	-25.5	112	143
Std-P+Std-S	108	-23.8	68	91

3.6 Film Test Results from Oven Aging

In order to confirm the coating thermal performance in the targeted application temperatures 100-200°C, 5 days aging was conducted in oven at 125°C, 150°C, 180°C and 200°C.

3.6.1 Weight Loss from Oven Aging %Weight loss of the 5 coating samples after 5 days aging at different temperatures were plotted in Figure 12. Compared with the lifetime prediction from Figure 8 based on TGA Arrhenius study, the behavior of DF-0009, HT-P and HT-S from film oven aging weight loss matches the prediction reasonably well considering the effect of arbitrarily set condition of TGA as discussed in section 3.4. DF-0009 and HT-S performed better than prediction only losing ~13% after 5 days of 200°C while prediction for 25% weight loss is ~5 days at 200°C for both coatings. HT-P and Std-S are close to the prediction losing ~20% after 5 days at 180°C while prediction for 25% weight loss is close to 180°C for these two coatings. The biggest discrepancy is Std-P and Std-S at the lower temperature range of 125°C and 150°C. At first look, the weight loss of these conventional coatings at lower temperature range are surprising much lower than prediction, equal or even lower than the high temperature resistant coatings. However from the next section showing property changes, it is clear that these conventional coatings suffered much more severe property deterioration than the high temperature resistant coatings at the whole temperature range including the low temperature data at 125°C and 150°C even with this short term 5 day testing.

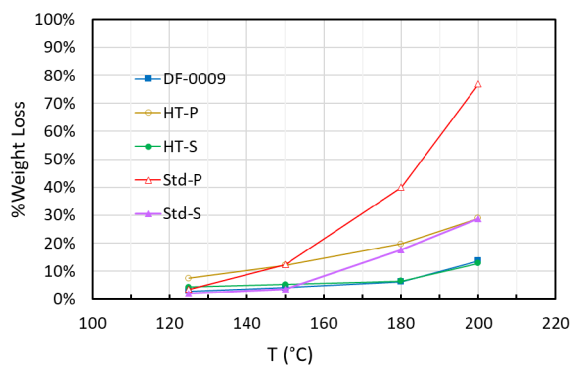


Figure 12. %Weight loss of coating film samples after 5 days in oven at different temperatures

This indicates weight loss from oven test is not a proper failure mode parameter that can represent the actual degree of polymer degradation at these lower temperatures. The cause of this discrepancy needs further investigation, only speculations can be assumed at this time. For example, the depolymerized species during short term under these lower temperature aging may not be small and volatile enough yet to release out even though properties already severely deteriorated. This is why measuring property change is more important to monitor the true progression of the coating degradation process at these relatively lower temperature ranges.

3.6.2 Change of Mechanical Properties Characterized by DMA

Both chain scission and crosslinking are directly associated with mechanical property changes of the polymeric materials after aging degradation. Chain scission causes reduction of crosslink density and it should be reflected in the equilibrium modulus E_0 (rubbery state modulus, directly proportional to crosslink density) drop from DMA. Crosslinking on the other hand causes crosslink density increase and it should result in increase of both T_g and E_0 . Figure 13 gives an example of DF-0009 DMA curves showing $Tan\delta$ peak shifting to higher temperature and the equilibrium modulus E_0

shifting higher after 5 days of 180°C aging, in agreement with crosslinking dominated degradation process.

The comparison of T_g increase is given in Figure 14. HT-S shows less T_g shift than DF-0009, which confirms the slightly better thermal stability of HT-S from Figure 7 TGA Arrhenius plot, both are much more stable than Std-S at high temperature level. Interestingly, T_g increase in Std-P is even less than HT-P, which may first appear not in agreement with its thermal stability being the worst, however, if considering Std-P is the only coating among these 5 coatings with chain scission being the dominant degradation mechanism, crosslinking being the minor one, this behavior of T_g shift not being so severe in Std-P can be easily understood. The true representation of the severe degradation occurred in Std-P is disclosed in Figure 15. After 5 days, Std-P lost equilibrium modulus $E_0 \sim 50\%$ after 125°C aging, $\sim 80\%$ after 150°C aging, until the reverse trend was seen modulus increased to be even higher than initial at 180°C. The temperature dependent behavior at a fixed time is equivalent to the time dependent behavior at a fixed temperature, which is in complete agreement with the observation in Figure 3 from Std-P/Std-S coated fiber at 180°C aging primary in-situ modulus first dropped to very low modulus gel state then increased to even much higher value than initial modulus. This confirms once again for conventional primary coating the degradation process progressed from early chain scission dominated stage to later crosslinking dominated stage. The softening and weakening of the material in the first chain scission dominated stage is most risky causing field failure such as attenuation increase and difficulty on handling due to easy tube off. It should be noted that even though the modulus increased to much higher level in the later crosslinking stage, the material is already severely embrittled with much lower elongation and toughness. For example, for Std-P film after 5 days 180°C with modulus appeared to be in similar level as initial film, the elongation at break dropped from initial 120% to 15%, a severely degraded material well passed any failure criteria.

HT-P although also showed minor decrease of E_0 from 4.2 to 3.4MPa after 5 days 125°C, it stayed far from getting into a gel-like stage. This confirms the 1st objective of the dual layer coating design, prevent the primary coating from undergoing severe chain scission to avoid disintegration into a gel-like material under high temperature applications, has been achieved. HT-S by showing the least T_g increase and negligible E_0 change after 5 days of the tested temperatures, similar behavior to DF-0009 and much better than Std-S, confirms the 2nd objective of the dual layer coating design, prevent the secondary coating from undergoing severe crosslinking to avoid detrimental embrittlement under high temperature applications, has also been achieved.

4. Conclusions

In this paper, the failure mechanism of the conventional urethane acrylate based dual layer coating for optical fiber under high temperature aging is proposed to be chain scission dominated primary coating disintegration and crosslinking dominated secondary coating embrittlement. A non-urethane acrylate based dual layer UV-curable coating system HT-P/HT-S with high temperature resistance has been developed. The evaluation of this new coating system based on the film properties characterized by TGA weight loss and DMA mechanical testing showed superior thermal stability at high temperature, much better than a standard coating system Std-P/Std-S, matching closely to the single coat high temperature coating DF-0009; furthermore, with the design of soft/hard dual layer coating system, this new generation dual layer high temperature resistant coating system is expected to provide much improved fiber performance such as strip force and microbending protection than the

current single coat product for specialty optical fiber applications under high temperature harsh environments.

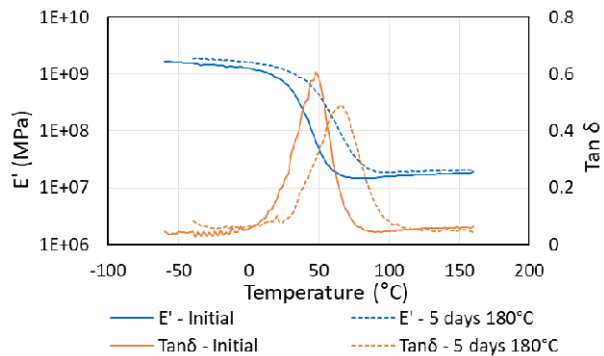


Figure 13. DMA loss modulus E' and $Tan\delta$ shift after 5 days in 180° oven for DF-0009 film samples

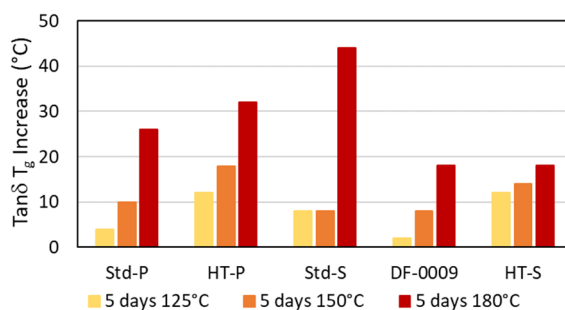


Figure 14. DMA T_g increase after 5 days in oven at different temperatures

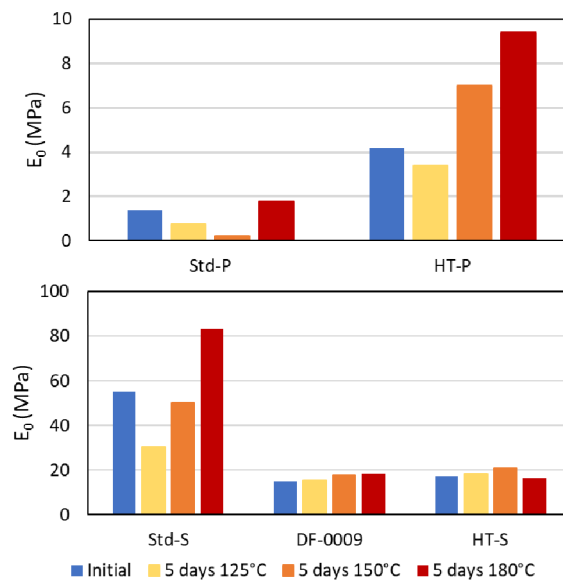


Figure 15. DMA equilibrium modulus E_0 of primary (top) and secondary/single coat (bottom) before and after 5 days in oven at different temperatures

5. References

- [1] E. Murphy, W. W. Catton, J. J. Kelly, “Improved Heat Resistant UV Cure Compositions for Optical Fiber Applications”, *Proc. 57th IWCS*, 197-201 (2008).
- [2] E. Murphy, P. Shah, J. J. Kelly, T. Anderson “New Heat Resistant UV Cure Coatings as Protective Overcoats for Optical Fiber Applications”, *Proc. 58th IWCS*, 90-94 (2009).
- [3] A. A. Stolov, D. A. Simoff, J. Li, “Thermal Stability of Specialty Optical Fibers”, *J. Lightwave Technology*, 26(20), 3443-3450 (2008).
- [4] D. A. Simoff, A. A. Stolov, C. R. Ciardiello, “New Optical Fiber Coating Designed for High-Temperature Applications”, *Proc. 58th IWCS*, 83-89 (2009).
- [5] A. A. Stolov, J. A. Wrubel, D. A. Simoff, R. J. Lago, “Acrylate-Based Specialty Optical Fiber Coatings for Harsh Environments”, *Proc. 65th IWCS*, 27-34 (2016).
- [6] P. A. M. Steeman, J. J. M. Slot, H. G. H. van Melick, A. A. F. v.d. Ven, H. Cao and R. Johnson, “Mechanical Analysis of the In-situ Primary Coating Modulus Test for Optical Fibers”, *Proc. 52nd IWCS*, 246-251 (2003).
- [7] P. Gijsman, *Handbook of Environmental Degradation of materials*, 2nd ed., p. 676 (2012).

6. Authors



Dr. Huimin Cao is a Science Fellow at Science and Technology Group at Covestro. Her expertise is material science, with the focus on material properties and structure-property relationships.



Todd Anderson is a Laboratory Technical Expert at Covestro Fiber Optic Materials Group. He has been working in the application process and testing of optical fiber coatings for over 20 years.



Keegan Orendorff is a Chemist at Covestro Fiber Optic Materials Group. He specializes in the production and analysis of UV materials with a focus on fiber optic coatings.



Dr. Eric Urruti is currently Head of R&D, North America, at Covestro. He has a diverse background encompassing research & development, manufacturing, and business management with a substantial record of successful new product introductions.



Covestro AG
Covestro Deutschland AG
Kaiser-Wilhelm-Allee 60
51373 Leverkusen
Germany

[covestro.com](https://www.covestro.com)

The manner in which you use our products, technical assistance and information (whether verbal, written or by way of production evaluations), including any suggested formulations and recommendations, is beyond our control. Therefore, it is imperative that you test our products to determine suitability for your processing and intended uses. Your analysis must at least include testing to determine suitability from a technical, health, safety, and environmental and regulatory standpoint. Such testing has not necessarily been done by Covestro, and Covestro has not obtained any approvals or licenses for a particular use or application of the product, unless explicitly stated otherwise. If the intended use of the product is for the manufacture of a pharmaceutical/medicinal product, medical device¹ or of pre-cursor products for medical devices or for other specifically regulated applications which lead or may lead to a regulatory obligation of Covestro, Covestro must explicitly agree to such application before the sale. Any samples provided by Covestro are for testing purposes only and not for commercial use. Unless we otherwise agree in writing, all products are sold strictly pursuant to the terms of our standard conditions of sale which are available upon request. All information, including technical assistance is given without warranty or guarantee and is subject to change without notice. It is expressly understood and agreed by you that you assume and hereby expressly release and indemnify us and hold us harmless from all liability, in tort, contract or otherwise, incurred in connection with the use of our products, technical assistance, and information. Any statement or recommendation not contained herein is unauthorized and shall not bind us. Nothing herein shall be construed as a recommendation to use any product in conflict with any claim of any patent relative to any material or its use. No license is implied or in fact granted under the claims of any patent. ¹Please see the "Guidance on Use of Covestro Products in a Medical Application" document.

Edition: September 2023